

Organic & Biomolecular Chemistry

Accepted Manuscript



This is an *Accepted Manuscript*, which has been through the Royal Society of Chemistry peer review process and has been accepted for publication.

Accepted Manuscripts are published online shortly after acceptance, before technical editing, formatting and proof reading. Using this free service, authors can make their results available to the community, in citable form, before we publish the edited article. We will replace this *Accepted Manuscript* with the edited and formatted *Advance Article* as soon as it is available.

You can find more information about *Accepted Manuscripts* in the [Information for Authors](#).

Please note that technical editing may introduce minor changes to the text and/or graphics, which may alter content. The journal's standard [Terms & Conditions](#) and the [Ethical guidelines](#) still apply. In no event shall the Royal Society of Chemistry be held responsible for any errors or omissions in this *Accepted Manuscript* or any consequences arising from the use of any information it contains.

**Computational rationalization of the selective C-H and C-F activations of
fluoroaromatic imines and ketones by cobalt complexes**

Jingjing Li, Dongju Zhang*, Hongjian Sun, and Xiaoyan Li*

*Key Lab of Colloid and Interface Chemistry, Ministry of Education, Institute of Theoretical
Chemistry, Shandong University, Jinan, 250100, P. R. China*

Corresponding authors:

1. Dr & Professor Dongju Zhang

E-mail: zhangdj@sdu.edu.cn

Phone: 86-531-88365833

Fax: 86-531-88564464

2. Dr & Professor Xiaoyan Li

E-mail: xli63@sdu.edu.cn

Phone: 86-531-88361350

Fax: 86-531-88564464

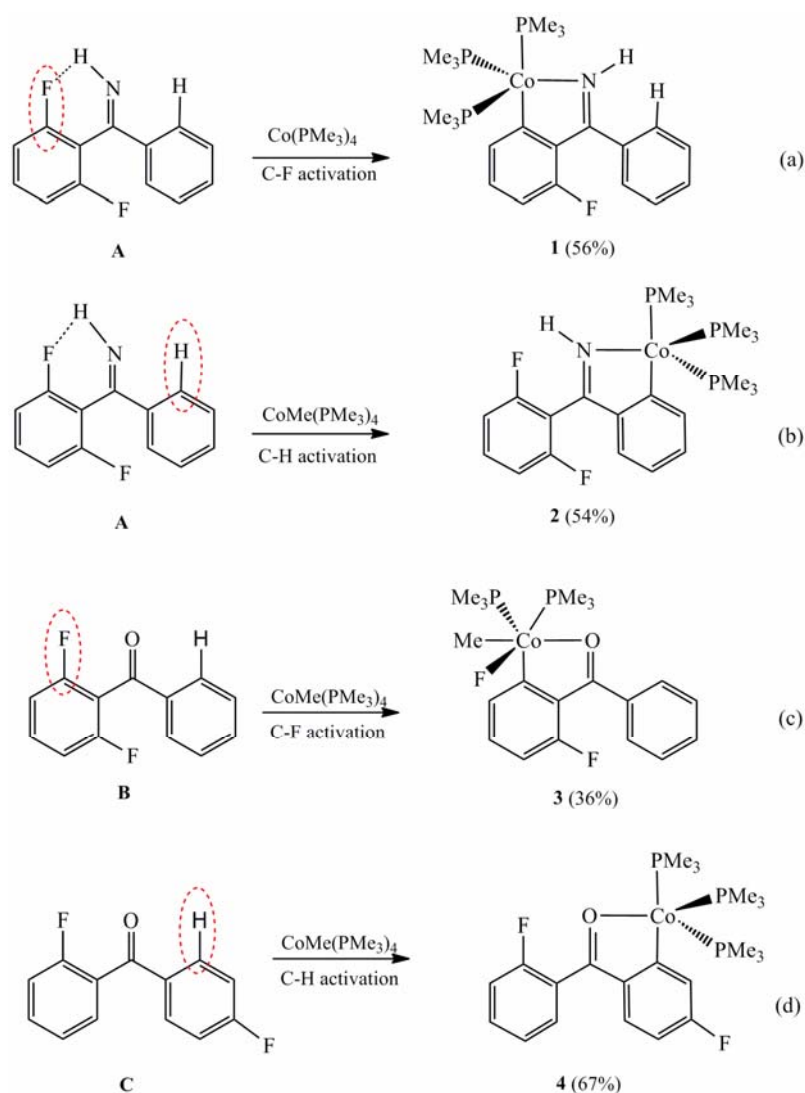
Abstract

While selective C-H and C-F activations of fluoroaromatic imines and ketones with transition metal complexes supported by PMe_3 have been successfully achieved in recent publications, insight into the molecular mechanism and energetics of those reactions is still lacking. Focusing on three typical substrates, 2,6-difluorobenzophenone imine (**A**) and 2,6-difluorobenzophenone (**B**), and 2,4'-difluorobenzophenone (**C**), the present work theoretically studied their C-H and C-F cyclometalation reactions promoted by activator $\text{Co}(\text{PMe}_3)_4$ or $\text{CoMe}(\text{PMe}_3)_4$. It is found that reaction **A** + $\text{Co}(\text{PMe}_3)_4$ favors the C-F activation, reaction **A** + $\text{CoMe}(\text{PMe}_3)_4$ prefers the C-H activation, whereas both the C-H and C-F activation pathways may be viable for reactions **B** + $\text{CoMe}(\text{PMe}_3)_4$ and **C** + $\text{CoMe}(\text{PMe}_3)_4$. The experimentally observed C-H and C-F cyclometalation products have been rationalized by analyzing the thermodynamic and kinetic properties of two activation pathways. From calculated results combined with the experimental observations, we believe that three factors, i.e. the oxidation state of metal center in the activators, the anchoring group of substrates, and substituted fluoroatom counts of aromatic ring in substrates, affect the selectivity of C-H and C-F activations of fluoroaromatic ketones and imines. Calculated results are enlightening to rational design of activators and substrates of fluoroaromatic imines and ketones to obtain exclusive C-H or C-F bond activation product.

1. Introduction

The selective activation of C-F and C-H bonds of fluoroaromatic compounds has attracted great attention in recent years mainly due to their potential use as starting materials for pharmaceuticals and agrochemicals.¹⁻⁴ In this field, transition metal complexes are the most widely used activators,⁵⁻⁸ some of which exclusively activate C-H bonds⁹⁻¹¹ and others are only effective at C-F bonds¹²⁻¹⁶. The activations of aryl C-F and C-H bonds *ortho* to a coordinating (anchoring) group are one of the most useful avenues functionalizing aromatic fluorocarbons in modern synthetic chemistry,¹⁷⁻²⁰ and a number of interesting examples have emerged over the past two decades.²¹⁻²⁶ Murai *et al.*²³ reported ruthenium catalyzed cleavage and addition of *ortho*-(C-H) bonds in aromatic ketones and imines. Barrio *et al.*²⁷ researched the selective C-H and C-F bond activations in the reactions of a hexahydride-osmium complex with aromatic ketones. They found that the ketone substrate containing only one aromatic ring prefer *ortho*-(C-H) bond activation to *ortho*-(C-F) bond activation while a reverse selectivity was observed for the ketone containing two aromatic groups (pentafluorobenzophenone), i.e. the C-F activation product was observed. Later on, Camadanli *et al.*²⁸ demonstrated that the selective C-F bond activation of pentafluorobenzophenone can be also achieved at low valence cobalt center. Yoshikai²⁹ systemically discussed cobalt-catalyzed C-H functionalization reactions, mainly involving alkenylation and alkylation reactions developed by his group. Recently, our group initiated a research project focusing on the selective activation of C-F and C-H bonds of fluoroaromatic ketones and imines compounds with iron, cobalt, and nickel complexes as activators³⁰⁻³² and obtained a series of promising products of C-F or C-H bond activation. Scheme 1 shows a representative example of our experimental results of the competitive C-F and C-H bond activations, where three substrates, 2,6-difluorobenzophenone imine (**A**), 2,6-difluorobenzophenone (**B**), and 2,4'-difluorobenzophenone (**C**), combine activator(s) $\text{Co}(\text{PMe}_3)_4$ (d^9 , 17 valence electrons) and/or $\text{CoMe}(\text{PMe}_3)_4$ (d^9 , 18 valence electrons) into

four situations: (a) **A** + $\text{Co}(\text{PMe}_3)_4$, (b) **A** + $\text{CoMe}(\text{PMe}_3)_4$, (c) **B** + $\text{CoMe}(\text{PMe}_3)_4$ and (d) **C** + $\text{CoMe}(\text{PMe}_3)_4$. It was found that (a) and (c) afford C-F activation products **1** with yield of 56% and **3** with yield of 36%, whereas (b) and (d) deliver the C-H activation products **2** with yield of 54% and **4** with yield of 67%.³⁰ These results are very valuable, which show promising methods selectively activating the C-F and C-H bonds of fluorinated aromatic ketones and imines.



Scheme 1. Selective C-H and C-F bond activations in the cyclometalation reactions of 2,6-difluorobenzophenone imine (**A**), 2,6-difluorobenzophenone (**B**), and 2,4'-difluorobenzophenone (**C**), using $\text{Co}(\text{PMe}_3)_4$ or $\text{CoMe}(\text{PMe}_3)_4$ as an activator, studied in our previous work.³⁰ The percentages below each structure is observed yields.

Despite these exciting results, insight into the molecular mechanism which controls the selectivity of C-F and C-H bond activations is not completely clear. To obtain a deeper understanding of observed selectivities, we here report a systematic theoretical study for all four reactions shown in Scheme 1. By carrying out density functional theory (DFT) calculations, we expect to (i) show the mechanism details of reactions at the molecular level, (ii) rationalize the experimental findings reported in our previous work, (iii) analyze the effects of the anchoring group, substituted fluoroatom counts in the aromatic ring, and the oxidation state of the activator on the selectivity, and (iv) provide guidance for experimenters who are paying attention on the selective activation of C-H and C-F bonds of aromatic fluorocarbons.

2. Computational details

All calculations were carried out using the Gaussian-03 software package³³ in the framework of density functional theory (DFT). The popular B3LYP functional³⁴⁻³⁷ was chosen due to its good performance for describing cobalt-containing organometallic systems.³⁸ Co atom was represented by the effective core potentials (ECPs) of Hay and Wadt with double- ξ valence basis sets (LanL2DZ).³⁹⁻⁴¹ The standard 6-31G (d, p) basis set was used for all other atoms. Full geometry optimizations were conducted without constraint, and vibrational frequency calculations were also carried out to verify all optimized structures as minima (zero imaginary frequencies) or first-order saddle points (one imaginary frequency) and to provide free energies at 298.15 K, which include entropic contributions by taking into account the vibrations, rotations, and translations of the structures. Transition states located were checked by performing the intrinsic reaction coordinate (IRC)^{42,43} calculations to confirm that each of them actually connects the desired reactant and product.

In the present work, our calculations have considered different spin states of each

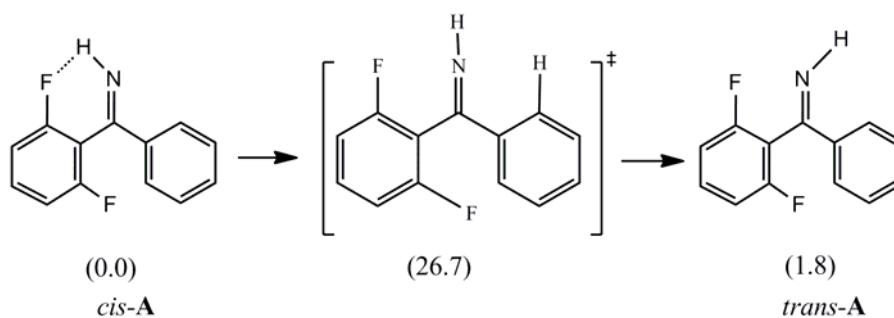
species of both the Co(0) and Co(I) systems. They are doublet and quartet states for situation (a) in Scheme 1, and the singlet and triplet states for situations (b), (c), and (d) in Scheme 1. In the following figures, only the structures involved in the energetically most favorable pathways were drawn out schematically for simplification.

To calibrate the quality of calculations in the present work, we compare calculated geometrical parameters of products **1**, **3** and **4** in Scheme 1 with corresponding X-ray diffraction values.³⁰ As shown in Table 1, theoretical geometrical parameters are in good agreement with experimental values, and the relative errors are in general smaller than 5% with an exception. These results make us confident about the reliability and accuracy of the level of theory used in the present work.

3. Results and discussion

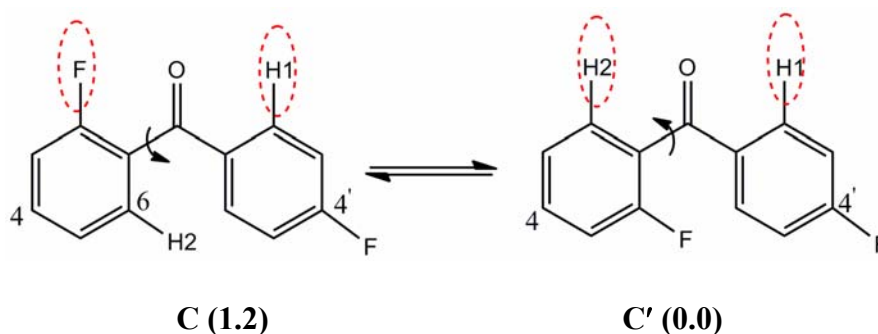
3.1 Substrates

Four reactions shown in Scheme 1 involve three isoelectronic substrates (**A**, **B**, and **C**) with planar geometries. Substrate **A** involves the imine anchoring group and has two distinct conformers, labeled as the *cis* and *trans*, depending on the imine H atom close or far away from the *ortho*-substituted F atom (Scheme 2). The *cis* conformer was found to be 1.8 kcal mol⁻¹ more stable than the *trans* one owing to its intramolecular hydrogen bonding. However, the calculated barrier for the transformation from the *cis* to *trans* is as high as 26.7 kcal mol⁻¹, implying that the *cis-trans* transformation may be difficult under thermal reaction conditions. Thus we believe that the *cis* conformer is preponderant. In the following calculations of relative energies, the energy of **A** always involves the *cis* conformer.



Scheme 2. Relative energies of *cis*- and *trans*-conformers of 2,6-difluorobenzophenone imine (A) and the barrier involved in the transformation from the *cis* to *trans*. Energies are in kcal mol⁻¹.

Substrates **B** and **C** have carbonyl as an anchoring group with different position of fluorine substitute. All these three substrates have both the C-F and C-H bonds *ortho* to the anchoring group (amine for **A** and carbonyl for **B** and **C**), allowing us compare their respective C-H versus C-F activation in the cyclometalation reaction with Co(PMe₃)₄ or CoMe(PMe₃)₄. However, it should be noted that 2,4'-difluorobenzophenone have two different configurations (**C** and **C'**, Scheme 3) which can change into each other via rotation about the C-CO bond, and only configuration **C** is relevant to the *ortho* C-F activation. Configuration **C'** is calculated to be the more stable by 1.2 kcal mol⁻¹ than **C**, indicating it is the preponderant configuration.



Scheme 3. Two different configurations (**C** and **C'**) of 2,4'-difluorobenzophenone resulted from rotation about the C-CO bond. The values in parentheses are calculated relative energies.

3.2 Reaction of 2,6-difluorobenzophenone imine (**A**) with $\text{Co}(\text{PMe}_3)_4$

The previous experiment³⁰ showed that treatment of **A** with $\text{Co}(\text{PMe}_3)_4$ affords the *ortho*-(C-F) bond activation product **1** with yield of 56%. To understand the observed selectivity of C-F bond activation, we performed calculations for this reaction along both *ortho*-(C-F) and *ortho*-(C-H) activation pathways. It is found that the lowest energy pathways involving both the C-F and C-H activation pathways occur on the doublet potential surface. Fig. 1 shows calculated free energy profiles, and Fig. 2 gives optimized geometries of intermediates (${}^2\mathbf{I}^{\mathbf{a}}$ - ${}^2\mathbf{VI}^{\mathbf{a}}$, the right superscript **a** means situation (a) in Scheme 1 and the left superscript **2** denotes the spin multiplicity. Similar expressions apply to all following symbols), and transition states (${}^2\mathbf{TS1}^{\mathbf{a}}$ - ${}^2\mathbf{TS3}^{\mathbf{a}}$).

Initially, along with the C-H activation pathway, σ -coordination of the nitrogen atom in *cis*-**A** to $\text{Co}(0)$ center of the activator with dissociation of a PMe_3 group from the metal center gives intermediate ${}^2\mathbf{I}^{\mathbf{a}}$, which is exothermic by $13.2 \text{ kcal mol}^{-1}$. Then, a new complex ${}^2\mathbf{II}^{\mathbf{a}}$ is obtained by dissociating a second PMe_3 group. Dissociation of these two PMe_3 groups is necessary to relieve steric hindrance and provide vacant site to the coming substrate. ${}^2\mathbf{II}^{\mathbf{a}}$ appears to be a direct precursor of C-H bond addition. The present calculations located a three-center transition state corresponding to C-H addition, ${}^2\mathbf{TS1}^{\mathbf{a}}$, which lies below the isolated reactants (**A** + $\text{Co}(\text{PMe}_3)_4$) by $0.6 \text{ kcal mol}^{-1}$ and above ${}^2\mathbf{I}^{\mathbf{a}}$ by $12.6 \text{ kcal mol}^{-1}$. The forwards product from ${}^2\mathbf{TS1}^{\mathbf{a}}$ corresponds to C-H addition product ${}^2\mathbf{III}^{\mathbf{a}}$, a 17-electron Co complex, which is more stable by $3.1 \text{ kcal mol}^{-1}$ than the isolated reactants. However, it should be noted that ${}^2\mathbf{III}^{\mathbf{a}}$ is less stable by $10.1 \text{ kcal mol}^{-1}$ than ${}^2\mathbf{I}^{\mathbf{a}}$, and moreover, the barrier ($12.6 \text{ kcal mol}^{-1}$) from ${}^2\mathbf{II}^{\mathbf{a}}$ to ${}^2\mathbf{III}^{\mathbf{a}}$ is much higher than that of the reverse process from ${}^2\mathbf{III}^{\mathbf{a}}$ to ${}^2\mathbf{I}^{\mathbf{a}}$ (12.6 vs $2.5 \text{ kcal mol}^{-1}$). In this sense, even if ${}^2\mathbf{III}^{\mathbf{a}}$ can be formed, it would immediately return to ${}^2\mathbf{II}^{\mathbf{a}}$ and then ${}^2\mathbf{I}^{\mathbf{a}}$. In other words, the C-H cyclometalation product may be not formed due to its high instability in energy.

We now explore the C-F bond activation pathway. To activate the *ortho*-(C-F) bond, ${}^2\mathbf{I}^a$ must be converted to another σ complex ${}^2\mathbf{IV}^a$, where the substrate moiety is in the *trans* configuration. ${}^2\mathbf{IV}^a$ is calculated to be less favorable in energy by 1.1 kcal mol⁻¹ than ${}^2\mathbf{I}^a$ due to loss of the intramolecular C-F...H hydrogen bond. This process proceeds via transition state ${}^2\mathbf{TS2}^a$ with a barrier of 14.4 kcal mol⁻¹, which is significantly lower than the barrier (26.7 kcal mol⁻¹, Scheme 2) for the transformation from the *cis* to *trans* without the assistance of the activator. Next, the dissociation of a second PMe₃ group from the metal center results in ${}^2\mathbf{V}^a$. Subsequently, the C-F oxidative addition to the Co center occurs via ${}^2\mathbf{TS3}^a$ with a barrier of 11.6 kcal mol⁻¹ to form C-F cyclometalation intermediate ${}^2\mathbf{VI}^a$, which can be further converted to the experimentally observed final product, **1** in Scheme 1 by losing F₂PMe₃ presumably through a bimolecular mechanism.³⁰ The released energy for the transformation from ${}^2\mathbf{I}^a$ to ${}^2\mathbf{VI}^a$ is calculated to be 21.6 kcal mol⁻¹, which is enough for compensating the energy required to break the C-F bond. So the huge thermodynamic stability of ${}^2\mathbf{VI}^a$ makes the reaction proceeds along the C-F bond activation pathway, which is in good agreement with the experimental observation³⁰.

3.3 Reaction of 2,6-difluorobenzophenone imine (A) with CoMe(PMe₃)₄

As shown in situation (b) in Scheme 1, C-H cyclometalation product **2** was observed with yield of 54% when CoMe(PMe₃)₄ was used as an activator. This is in contrast with situation (a) discussed above which used Co(PMe₃)₄ as the activator and led to C-F cyclometalation product **1**. This fact clearly indicates that the oxidation state of Co center in the activator plays an intrinsic role for the selective activation of *ortho* C-F and C-H bonds. To understand the molecular mechanism, we carried out calculations along both C-H and C-F activation pathways on both the singlet and doublet surfaces. It was found that the most favorable C-H and C-F activation pathways occur on the singlet and doublet surfaces, respectively. Fig. 3 gives calculated free energy profiles and Fig. 4 shows optimized geometries of intermediates

and transition states involved.

Similar to situation (a) discussed above, the reaction initiates via coordination of *cis*-**A** to Co(I) center to successively form σ -complexes $^3\mathbf{I}^b$, $^1\mathbf{II}^b$ and $^3\mathbf{II}^b$ with dissociation of one and two PMe_3 groups. As shown Fig. 3, the formations of $^1\mathbf{II}^b$ and $^3\mathbf{II}^b$ are exothermic by 19.0 and 37.8 kcal mol⁻¹, respectively. Along the C-H bond activation pathway on the singlet surface, $^1\mathbf{II}^b$ is converted to the final product **2** via two elementary steps: the oxidation addition of C-H bond followed by the reductive elimination of CH_4 . The former proceeds via transition state $^1\mathbf{TS1}^b$ to form $^1\mathbf{III}^b$, a methyl hydrido complex of Co(III), and the latter occurs via $^1\mathbf{TS2}^b$ to lead to $^1\mathbf{IV}^b$, which then associates a PMe_3 group to form the final product **2**, an 18-electron complex. The overall barrier for the C-H activation is calculated to be 14.7 kcal mol⁻¹, and the whole reaction is exothermic by 38.9 kcal mol⁻¹.

Alternatively, along the C-F bond activation pathway on the triplet surface, $^3\mathbf{II}^b$ must first be converted into $^3\mathbf{V}^b$ via $^3\mathbf{TS3}^b$ with a barrier of 28.0 kcal mol⁻¹, and subsequently the Co(I) center in $^3\mathbf{V}^b$ inserts into the *ortho*-(C-F) bond with a barrier of 12.9 kcal mol⁻¹, leading to C-F cyclometalation intermediate $^3\mathbf{VI}^b$. However, it is found that the ground state of \mathbf{VI}^b is in its singlet state and to lie below the reactants by 42.0 kcal mol⁻¹. So we conjecture that there is a spin-crossover transition from $^3\mathbf{VI}^b$ to $^1\mathbf{VI}^b$ along the C-F activation pathway.

Obviously, the transformation from $^3\mathbf{II}^b$ to $^3\mathbf{V}^b$ is the rate-determining step of the C-F activation pathway, and its barrier (28.0 kcal mol⁻¹) is too high to be overcome at room temperature. As a consequence, the reaction preferably proceeds along the C-H activation pathway, leading to the experimentally observed C-H cyclometalation product **2**.

We now compare situations (a) and (b) shown in Scheme 1, which use the same substrate (**A**) and similar but different activators ($\text{Co}(\text{PMe}_3)_4$ and $\text{CoMe}(\text{PMe}_3)_4$, respectively). For situation (a) (Fig. 1) the selective activation of C-F bond can be understood according to the huge difference of thermodynamic stability of C-F and C-H cyclometalation complexes, $^2\mathbf{VI}^a$ and $^2\mathbf{III}^a$, (-34.8 vs -3.1 kcal mol⁻¹). In distinct contrast, the selectivity pattern in situation (b)

(Fig. 3) is inverted and the C-H activation product is obtained. This fact is attributed to both the high barrier involved along the C-F activation pathway, and the high stability of **2** (18-electron complex) in comparison with its analogue **III^a** (17-electron complex) in Fig. 1.

From above discussion, it is clear that the oxidation state of Co center plays an intrinsically important role for the selective *ortho* C-F and C-H activations of fluoroaromatic imines: Co(0) promotes the C-F activation while Co(I) favors the C-H bond activation.

3.4 Reaction of 2,6-difluorobenzophenone (**B**) with CoMe(PMe₃)₄

Our attention now turns to situation (c) in Scheme 1, the reaction of **B** with CoMe(PMe₃)₄. Fig. 5 shows calculated free energy profiles on the singlet and triplet surfaces for the C-H and C-F bond activations, and Fig. 6 gives optimized geometries of stationary points on the potential energy surface. Initially, **B** coordinates to the Co(I) center via its carbonyl O atom to form the σ -complex **³I^c** (exothermic by 18.3 kcal mol⁻¹) with departure of a PMe₃ ligand. **³I^c** then evolves into **¹III^c**, a less stable common precursor of C-H activation, or into **³II^c**, a more stable precursor of C-F activation via dissociation of a second PMe₃ group from the metal center.

For the C-H bond activation, the calculated mechanism is very similar to that in situation (b): the reaction proceeds via two elementary steps, the C-H bond oxidation addition followed by the reductive elimination of CH₄, leading to the C-H cyclometalation product. The whole reaction is exothermic by 42.3 kcal mol⁻¹ with an overall barrier of 17.1 kcal mol⁻¹ (the energy difference between **¹TS3^c** and **³I^c**). Alternatively, along the C-F bond activation pathway, **³II^c** may immediately evolve to the stable C-F activation product **³3** via **³TS1^c** with a barrier of 18.1 kcal mol⁻¹. Similar to the reaction of CoMe(PMe₃)₄ with **A** discussed above, there is a spin-crossover transition from **³3** to **¹3** at the exit of reaction to obtain the most stable ground state product.

Both the C-H and C-F activations involve low and comparative barriers as well as high

reaction heats. So from an energetic point of view, it seems that both the C-H and C-F activation pathways are viable at room temperature. This can explain the low yield (36%) of the C-F activation product (**3** in Scheme 1) observed in the experiment.³⁰ In other words, when the imine group in substrate is replaced by the iso-electronic carbonyl, the selectivity of the reaction becomes lower. The imine group that forms an intramolecular hydrogen bond with the *ortho* C-F bond (Scheme 2) and hence impedes the C-F bond activation and favors the C-H bond activation. Therefore, the imine group is the better anchoring group than the keto group, which agrees with the experimental finding.³⁰

3.5. Reaction of 2,4'-difluorobenzophenone (**C**) with $\text{CoMe}(\text{PMe}_3)_4$

For situation (d) in Scheme 1, the reaction of 2,4'-difluorobenzophenone with $\text{CoMe}(\text{PMe}_3)_4$, the calculated results along the energetically most favorable pathways are given in Figs. 7 and 8. Substrate **C** is a structural isomer of **B**, which contains two mono-fluorinated aromatic ring. The mechanism obtained from the present calculations is similar to the reaction of 2,6-difluorobenzophenone (situation (c) in Scheme 1.). The C-H and C-F activations proceed on the singlet and triplet surfaces, respectively. The calculated barriers and reaction energies are 13.2 and 33.2 kcal mol⁻¹ for the former, and 13.7 and 40.3 kcal mol⁻¹ for the latter. Two pathways involve low and comparative barriers and reaction heats. Therefore, both the C-H and C-F activation pathways are viable at room temperature. This result seems not to be consistent with the experimentally reported C-H activation product (**4** in Scheme 1) with yield of 67%.

However, it should be noted that there exist two equivalent configurations for 2,4'-difluorobenzophenone, as shown by **C** and **C'** in Scheme 3. These two configurations can interconvert into each other through rotation of the C-CO bond at room temperature. Configuration **C'**, which is energetically more favorable than **C** by 1.2 kcal mol⁻¹, is the preponderant configuration. In **C'**, there are two *ortho* hydrogen atoms (H1 and H2) around

the anchoring group. Thus the reaction of 2,4'-difluorobenzophenone actually involves three possible pathways: C-F activation and C-H1 and C-H2 activations. In this sense, the probability of C-H activation is much larger than that of C-F activation. So the experiment observed the C-H activation product (**4** in Scheme 1), which corresponds to C-H1 activation. Our calculations show that the barrier along the C-H1 activation pathway is lower by 2.0 kcal mol⁻¹ than that of the C-H2 activation pathway. Compared to situation (c) in Scheme 1, it is clear that reducing substituted fluoroatom counts in the phenyl ring make the *ortho* C-F bond activation more difficult. In particular, the absence of F atom at C6 position in 2,4'-difluorobenzophenone reduces the C-F activation possibility.

4. Conclusive remarks

In conclusion, detailed DFT calculations have been carried on the C-H and C-F cyclometalation reactions of three typical substrates of fluoroaromatic imines and ketones, **A**, **B**, and **C** promoted by activator Co(PMe₃)₄ or CoMe(PMe₃)₄. Substrate **A** involving imine anchoring group evolves into the C-F activation product as using the zero-valence cobalt activator, but into the C-H activation product as using one-valence cobalt activator. In contrast, for substrates **B** and **C** involving keto anchoring group, as combined with the one-valence cobalt activator, both the C-H and C-F activations seem to be viable from the present calculations, which is in good agreement that the experimental finding that imine group is the better anchoring group than the keto group. Our calculations confirm that the oxidation state of metal center in the activator and the anchoring group in substrates intrinsically influence the selectivity of C-H and C-F bonds of fluoroaromatic ketones and imines. The theoretical data are enlightening to rational design of activators and substrates of fluoroaromatic imines and ketones toward the “targeted” C-H or C-F bond activation.

Acknowledgment. We greatly thank National Natural Science Foundation of China (NSFC

21273131 and 21172132) for support of this work.

Electronic supplementary information (ESI) available: Descartes coordinates for all geometries optimized in this work.

References:

- 1 S. A. Johnson, C. W. Huff, F. Mustafa and M. Saliba, *J. Am. Chem. Soc.*, 2008, **130**, 17278-17280.
- 2 E. Clot, O. Eisenstein, N. Jasim, S. A. Macgregor, J. E. McGrady and R. N. Perutz, *Acc. Chem. Res.*, 2011, **44**, 333-348.
- 3 A. Jana, P. P. Samuel, G. Tavcar, H. W. Roesky and C. Schulzke, *J. Am. Chem. Soc.*, 2010, **132**, 10164-10170.
- 4 D. Yu, L. Lu and Q. Shen, *Org. Lett.*, 2013, **15**, 940-943.
- 5 D. Alberico, M. E. Scott and M. Lautens, *Chem. Rev.*, 2007, **107**, 174-238.
- 6 G. Dyker, *Angew. Chem., Int. Ed.*, 1999, **38**, 1698-1712.
- 7 M. Zhou, U. Hintermair, B. G. Hashiguchi, A. R. Parent, S. M. Hashmi, M. Elimelech, R. A. Periana, G. W. Brudvig and R. H. Crabtree, *Organometallics.*, 2013, **32**, 957-965.
- 8 A. H. Klahn, B. Oelckers, F. Godoy, M. T. Garland, A. Vega, R. N. Perutz and C. L. Higgitt, *J. Chem. Soc., Dalton Trans.*, 1998, **18**, 3079-3086.
- 9 K. Wada, C. B. Pamplin, P. Legzdins, B. O. Patrick, I. Tsyba and R. Bau, *J. Am. Chem. Soc.*, 2003, **125**, 7035-7048.
- 10 E. Ben-Ari, R. Cohen, M. Gandelman, L. J. W. Shimon, J. M. L. Martin and D. Milstein, *Organometallics.*, 2006, **25**, 3190-3210.
- 11 D. Balcells, E. Clot and O. Eisenstein, *Chem. Rev.*, 2010, **110**, 749-823.
- 12 S. A. Johnson, E. T. Taylor and S. J. Cruise, *Organometallics.*, 2009, **28**, 3842-3855.
- 13 T. Braun and R. N. Perutz, *Chem. Commun.*, 2002, **23**, 2749-2757.

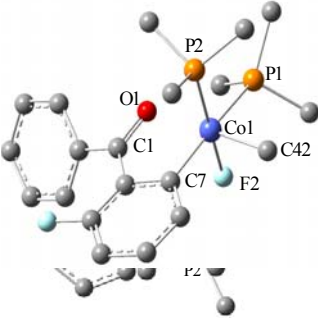
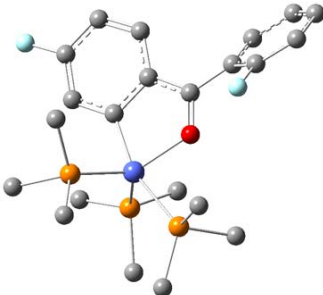
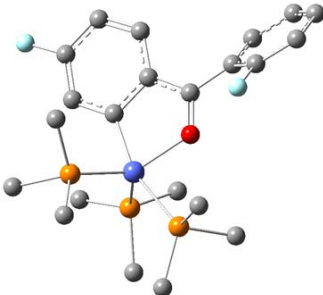
- 14 A. Nova, M. Reinhold, R. N. Perutz, S. A. Macgregor and J. E. McGrady, *Organometallics.*, 2010, **29**, 1824-1831.
- 15 A. L. Raza, J. A. Panetier, M. Teltewskoi, S. A. Macgregor and T. Braun, *Organometallics.*, 2013, **32**, 3795-3807.
- 16 A. D. Sun and J. A. Love, *Dalton Trans.* 2010, **39**, 10362-10374.
- 17 V. Ritleng, C. Sirlin and M. Pfeffer, *Chem. Rev.*, 2002, **102**, 1731-1770.
- 18 N. M. Brunkan, D. M. Brestensky and W. D. Jones, *J. Am. Chem. Soc.*, 2004, **126**, 3627-3641.
- 19 A. L. Keen, M. Doster, H. Han and S. A. Johnson, *J. Am. Chem. Soc.*, 2006, **128**, 1806-1807.
- 20 K. Fuchibe and T. Akiyama, *J. Am. Chem. Soc.*, 2006, **128**, 1434-1435.
- 21 S. Murai, F. Kakiuchi, S. Sekine, Y. Tanaka, A. Kamatani, M. Sonoda and N. Chatani, *Nature.*, 1993, **366**, 529-531.
- 22 F. Kakiuchi and S. Murai, *Acc. Chem. Res.*, 2002, **35**, 826-834.
- 23 F. Kakiuchi, S. Kan, K. Igi, N. Chatani and S. Murai, *J. Am. Chem. Soc.*, 2003, **125**, 1698-1699.
- 24 F. Kakiuchi, Y. Matsuura, S. Kan and N. Chatani, *J. Am. Chem. Soc.*, 2005, **127**, 5936-5945.
- 25 F. Kakiuchi, M. Usui, S. Ueno, N. Chatani and S. Murai, *J. Am. Chem. Soc.*, 2004, **126**, 2706-2707.
- 26 S. Hiroshima, D. Matsumura, T. Kochi and F. Kakiuchi, *Org. Lett.*, 2010, **12**, 5318-5321.
- 27 P. Barrio, R. Castarlenas, M. A. Esteruelas, A. Lledós, F. Maseras, E. Oñate and J. Tomàs. *Organometallics.*, 2001, **20**, 442-452.
- 28 S. Camadanli, R. Beck, U. Flörke and H. -F. Klein, *Dalton Trans.*, 2008, **42**, 5701-5704.
- 29 N. Yoshikai, *Synlett.*, 2011, **8**, 1047-1051.
- 30 T. Zheng, H. Sun, J. Ding, Y. Zhang and X. Li, *J. Organomet. Chem.*, 2010, **695**,

1873-1877.

- 31 J. Li, T. Zheng, H. Sun, W. Xu and X. Li, *Dalton Trans.*, 2013, **42**, 5740-5748.
- 32 X. Xu, J. Jia, H. Sun, Y. Liu, W. Xu, Y. Shi, D. Zhang and X. Li, *Dalton Trans.*, 2013, **42**, 3417-3428.
- 33 Revision D.01, M. J. Frisch, G. W. Trucks, H. B. Schlegel, G. E. Scuseria, M. A. Robb, J. R. Cheeseman, J. A. Montgomery Jr, T. Vreven, K. N. Kudin, J. C. Burant, J. M. Millam, S. S. Iyengar, J. Tomasi, V. Barone, B. Mennucci, M. Cossi, G. Scalmani, N. Rega, G. A. Petersson, H. Nakatsuji, M. Hada, M. Ehara, K. Toyota, R. Fukuda, J. Hasegawa, M. Ishida, T. Nakajima, Y. Honda, O. Kitao, H. Nakai, M. Klene, X. Li, J. E. Knox, H. P. Hratchian, J. B. Cross, V. Bakken, C. Adamo, J. Jaramillo, R. Gomperts, R. E. Stratmann, O. Yazyev, A. J. Austin, R. Cammi, C. Pomelli, J. W. Ochterski, P. Y. Ayala, K. Morokuma, G. A. Voth, P. Salvador, J. J. Dannenberg, V. G. Zakrzewski, S. Dapprich, A. D. Daniels, M. C. Strain, O. Farkas, D. K. Malick, A. D. Rabuck, K. Raghavachari, J. B. Foresman, J. V. Ortiz, Q. Cui, A. G. Baboul, S. Clifford, J. Cioslowski, B. B. Stefanov, G. Liu, A. Liashenko, P. Piskorz, I. Komaromi, R. L. Martin, D. J. Fox, T. Keith, M. A. Al-Laham, C. Y. Peng, A. Nanayakkara, M. Challacombe, P. M. W. Gill, B. Johnson, W. Chen, M. W. Wong, C. Gonzalez, J. A. Pople, Gaussian, Inc., Wallingford CT, 2004.
- 34 A. D. Becke, *Phys. Rev. A.*, 1988, **38**, 3098-3100.
- 35 C. Lee, W. Yang and R. G. Parr, *Phys. Rev. B.*, 1988, **37**, 785-789.
- 36 A. D. Becke, *J. Chem. Phys.*, 1993, **98**, 5648-5652.
- 37 B. Miehlich, A. Savin, H. Stoll and H. Preuss, *Chem. Phys. Lett.*, 1989, **157**, 200-206.
- 38 N. Godbout and E. Oldfield, *J. Am. Chem. Soc.*, 1997, **119**, 8065-8069.
- 39 P. J. Hay and W. R. Wadt, *J. Chem. Phys.*, 1985, **82**, 270-283.
- 40 P. J. Hay and W. R. Wadt, *J. Chem. Phys.*, 1985, **82**, 299-310.
- 41 W. R. Wadt and P. J. Hay, *J. Chem. Phys.*, 1985, **82**, 284-298.
- 42 K. Fukui, *J. Phys. Chem.*, 1970, **74**, 4161-4163.

43 K. Fukui, *Acc. Chem. Res.*, 1981, **14**, 363-368.

Table 1. Calculated and experimental bond distances (in Å) of C-H and C-F cyclometalation products.^a

	bond	r_{calc}^b	r_{expt}^c	Δr^d	Δr^e
 <p>1</p>	Co1-N1	1.940	1.885	0.055	2.8%
	Co1-P2	2.263	2.190	0.073	3.2%
	Co1-P3	2.250	2.200	0.050	2.2%
	Co1-P4	2.301	2.216	0.085	3.7%
	C1-Co1	1.963	1.936	0.027	1.4%
	C7-N1	1.321	1.336	0.015	1.1%
 <p>3</p>	Co1-C7	1.928	1.895	0.033	1.7%
	Co1-F2	1.852	1.932	0.080	4.1%
	Co1-O1	2.114	2.021	0.093	4.4%
	Co1-P1	2.265	2.212	0.053	2.3%
	Co1-P2	2.408	2.214	0.194	8.1%
	Co1-C42	1.963	1.995	0.032	1.6%
	O1-C1	1.252	1.247	0.005	0.4%
	P3-Co1	2.240	2.189	0.051	2.3%
	P2-Co1	2.322	2.227	0.095	4.1%
	P1-Co1	2.230	2.184	0.046	2.1%
 <p>4</p>	Co1-O1	2.000	1.905	0.095	4.8%
	Co1-C1	1.936	1.921	0.015	0.8%

^aThe hydrogen atoms in each structure have been omitted for clarity, and distances are given in Å. ^bcalculated values. ^cexperimental values. ^dabsolute errors. ^erelative errors.

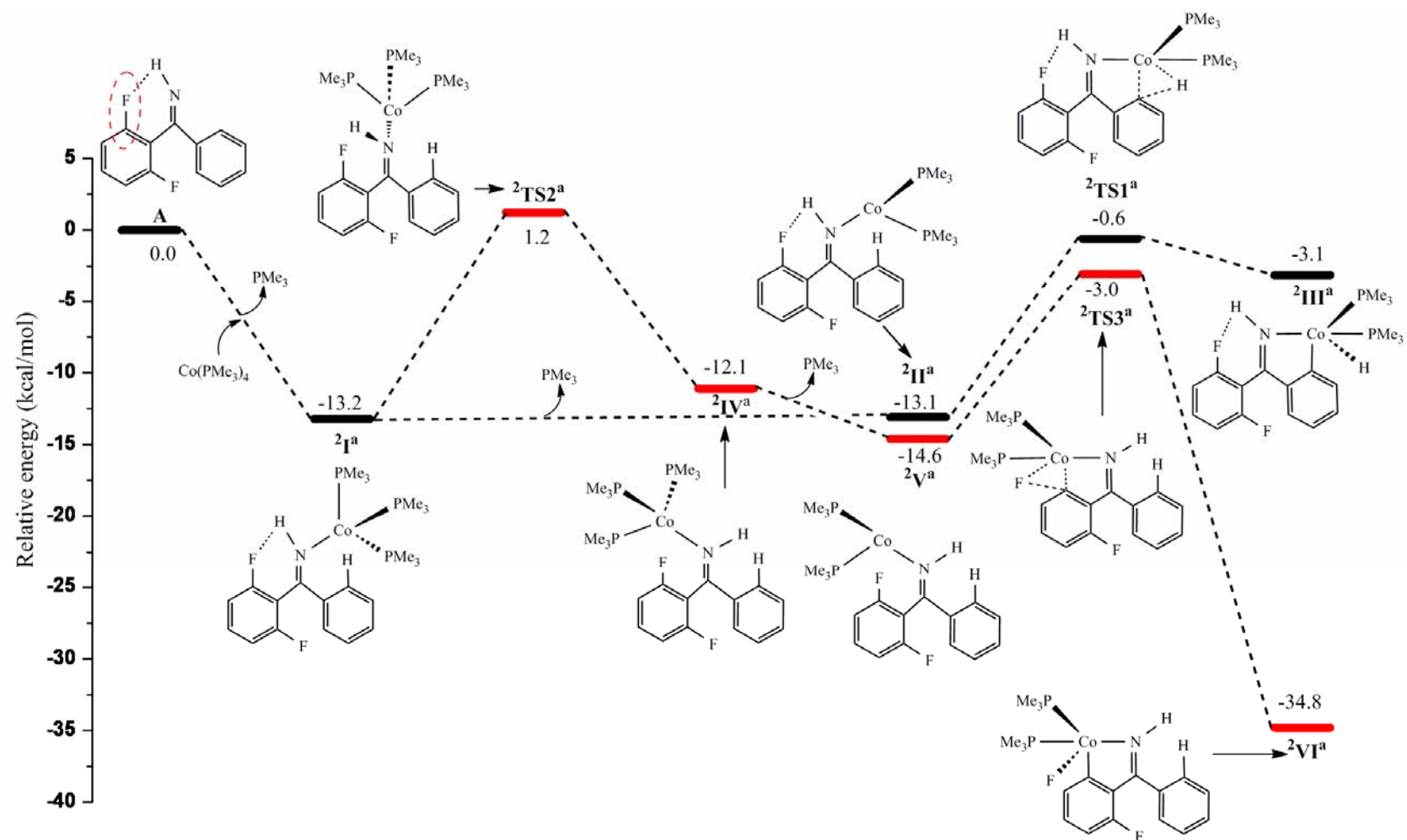


Fig. 1 Calculated free energy profiles on the doublet potential energy surface for the reaction of 2,6-difluorobenzophenone imine (**A**) with $\text{Co}(\text{PMe}_3)_4$ along both the *ortho* C-F activation pathway (red line) and the *ortho* C-H activation pathway (black line).

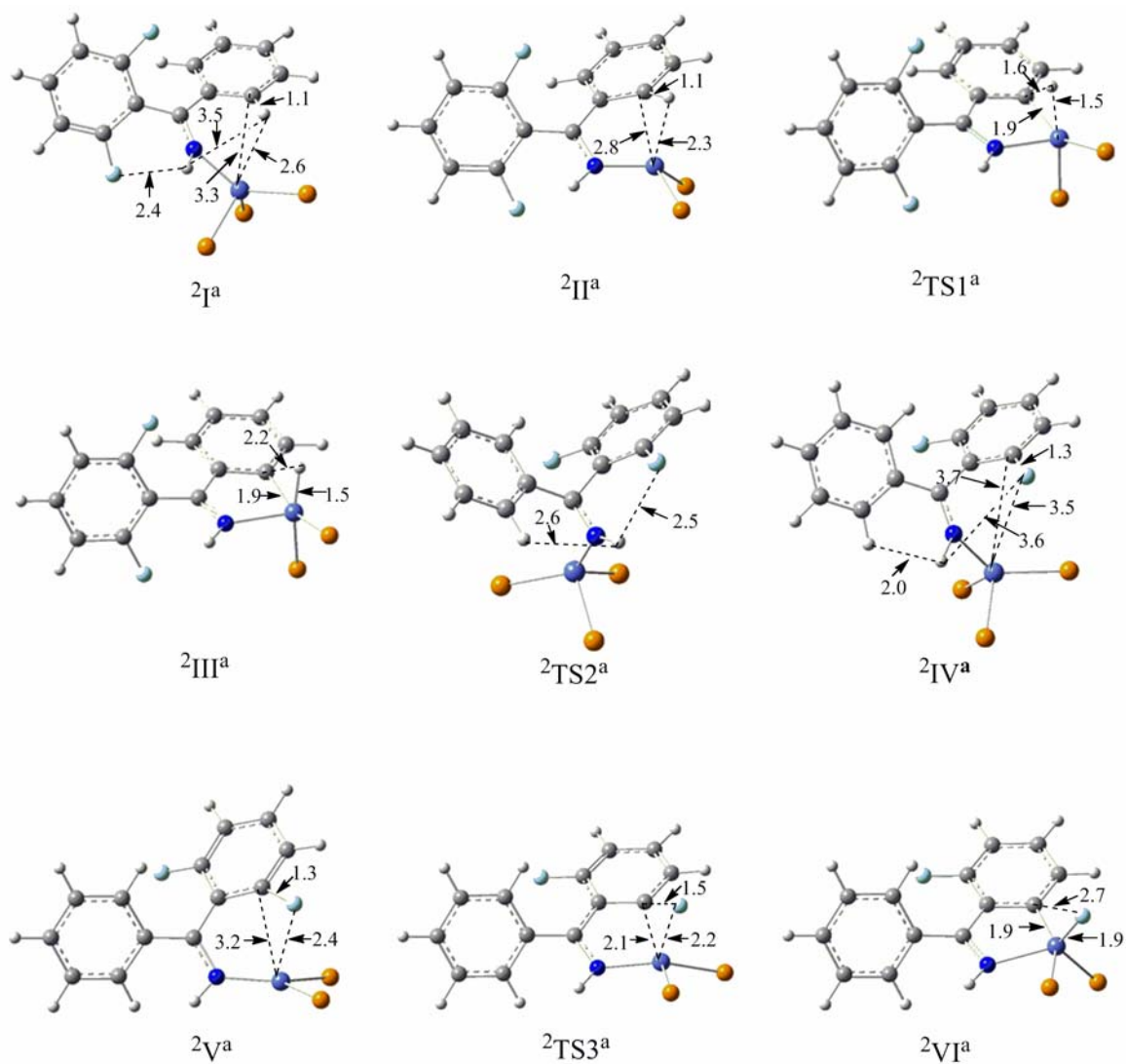


Fig. 2 Optimized structures with crucial geometrical parameters (in Å) for all schematic structures involved in Fig. 1. The methyl groups on phosphorous atoms have been omitted for clarity, and bond distances are given in Å.

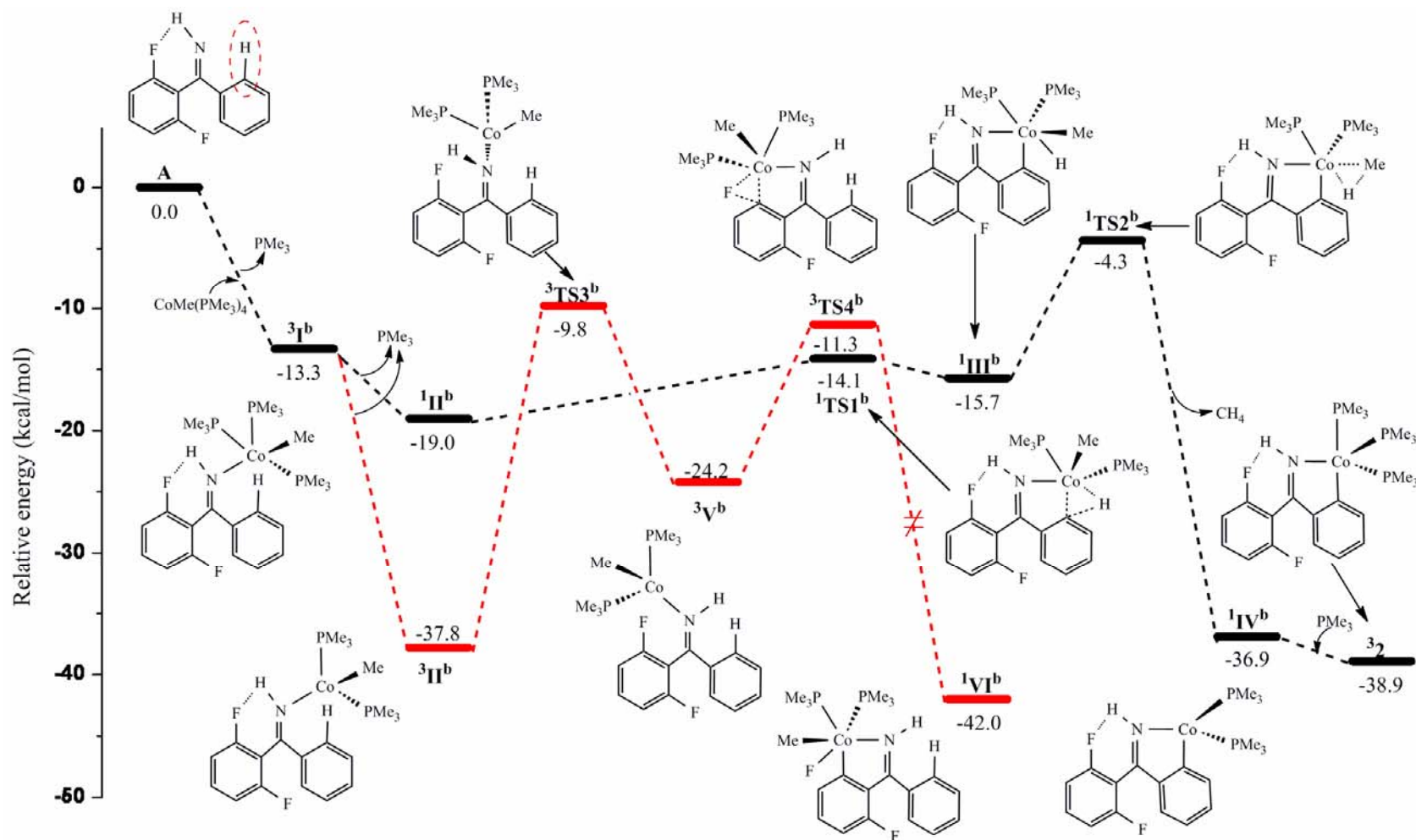


Fig. 3 Calculated free energy profiles for the reaction of $\text{CoMe}(\text{PMe}_3)_4$ with 2,6-difluorobenzophenone imine (A) along both the *ortho* C-F activation pathway (red line) on the triplet surface and the *ortho* C-H activation pathway (black line) on the singlet surface. The symbol \neq denotes the spin-crossover transition from the triplet surface to the singlet surface.

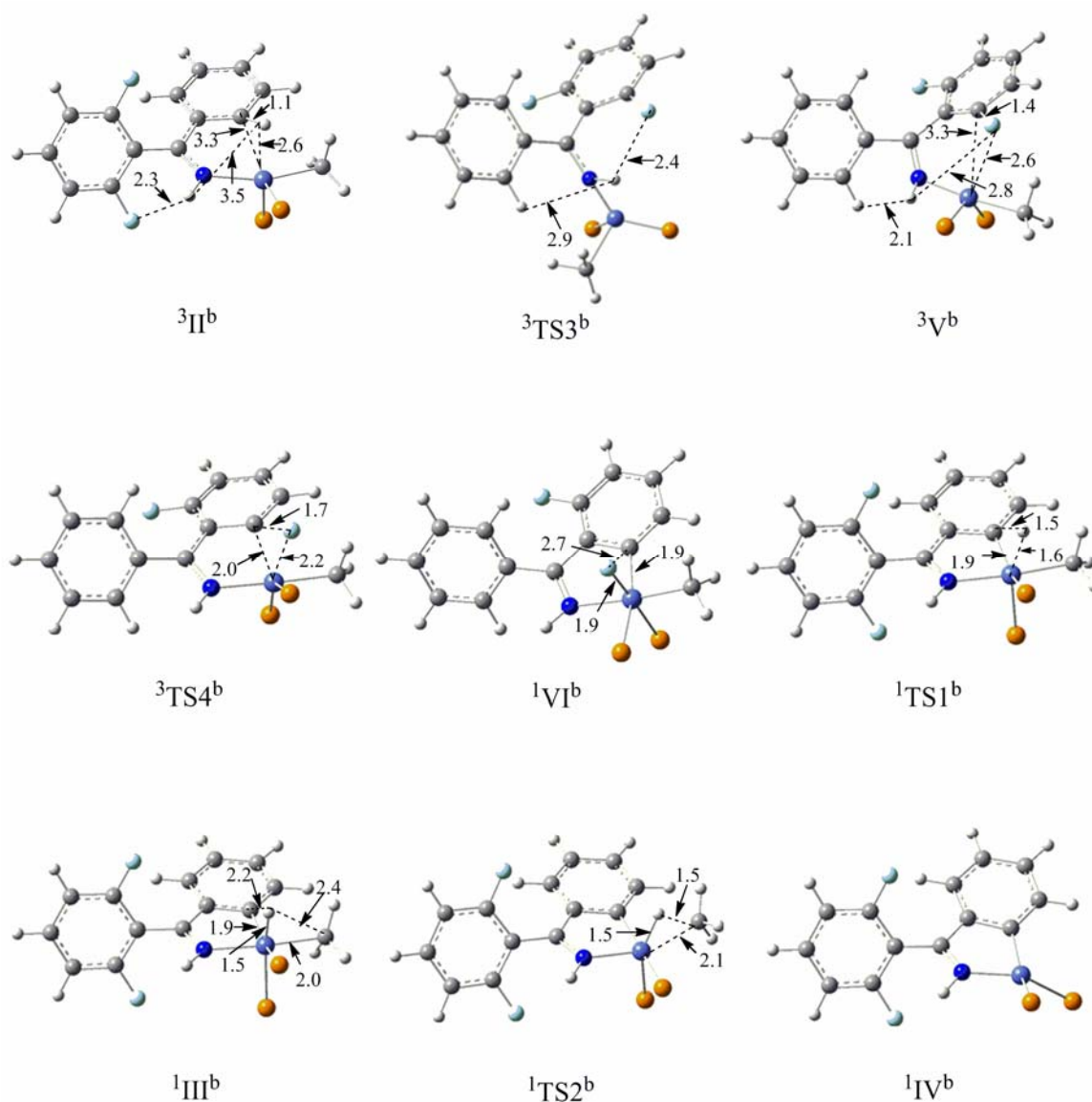


Fig. 4 Optimized structures with crucial geometrical parameters (in Å) for all schematic structures involved in Fig. 3. The methyl groups on phosphorous atoms have been omitted for clarity, and bond distances are given in Å.

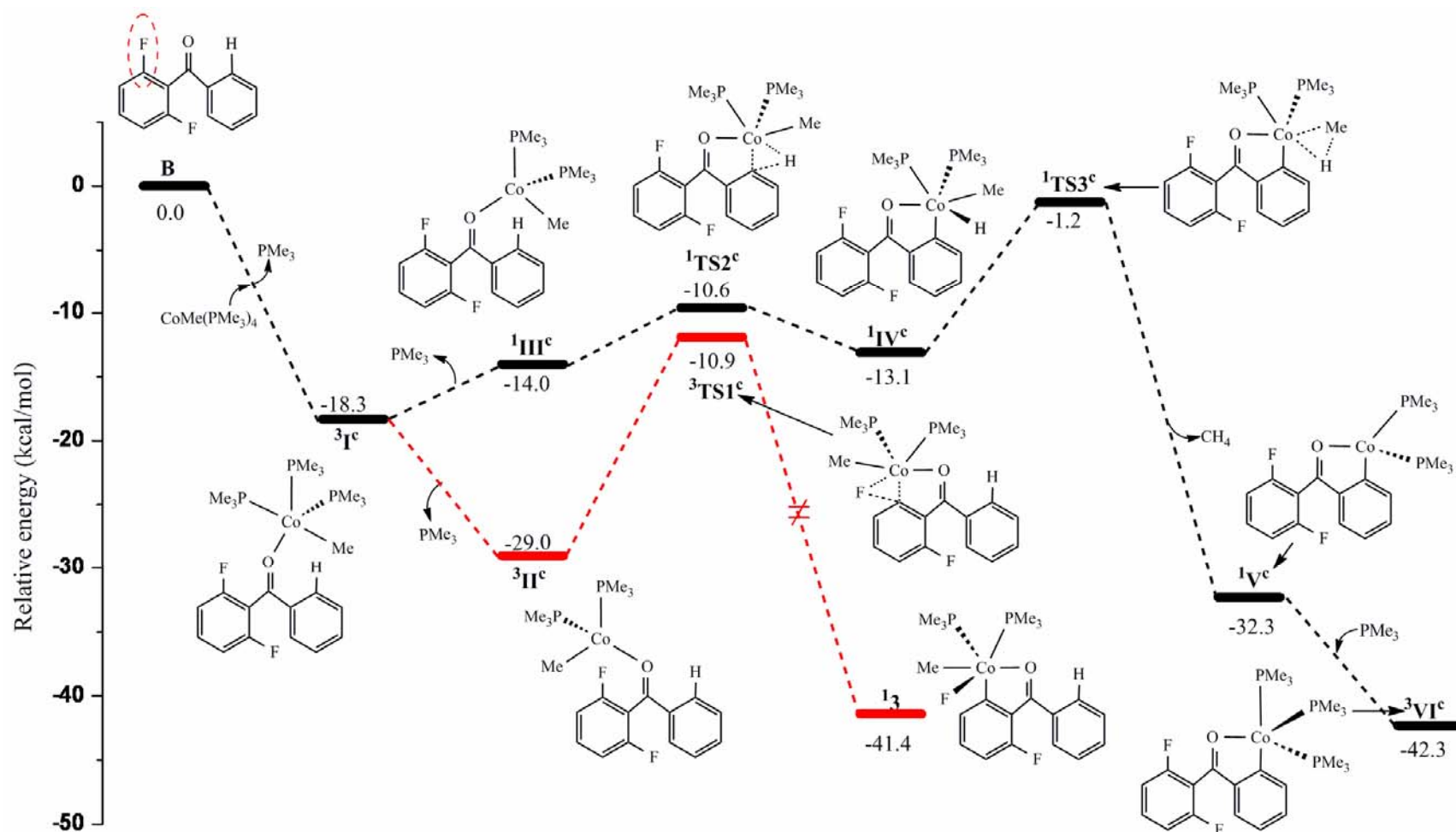


Fig. 5 Calculated free energy profiles for the reaction of $\text{CoMe(PMe}_3)_4$ with 2,6-difluorobenzophenone (**B**) along both the *ortho* C-F activation pathway (red line) and the *ortho* C-H activation pathway (black line). The symbol \neq denotes the spin-crossover transition from the triplet surface to the singlet surface.

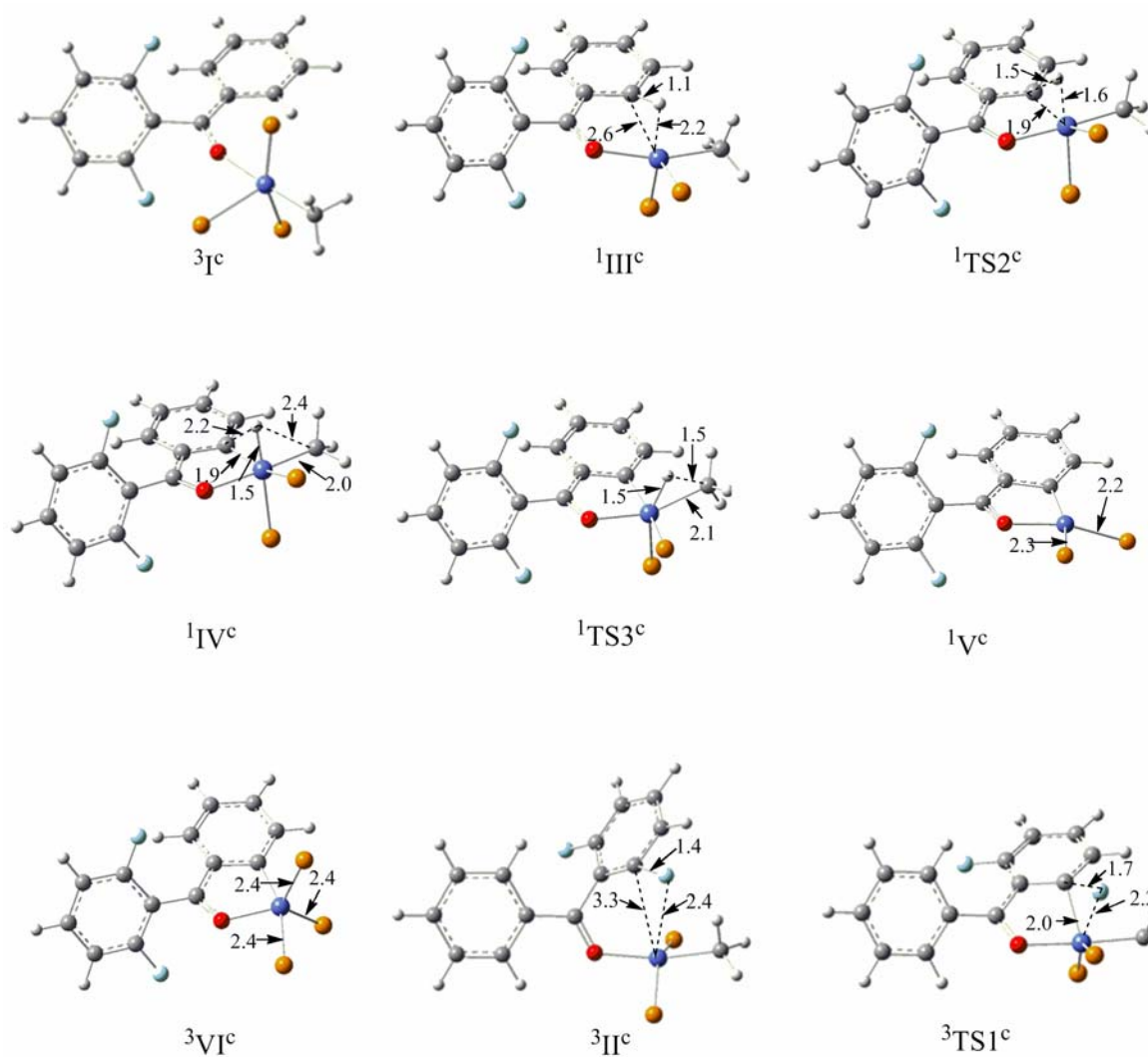


Fig. 6 Optimized structures with crucial geometrical parameters (in Å) for all schematic structures involved in Fig. 5. The methyl groups on phosphorous atoms have been omitted for clarity, and bond distances are given in Å.

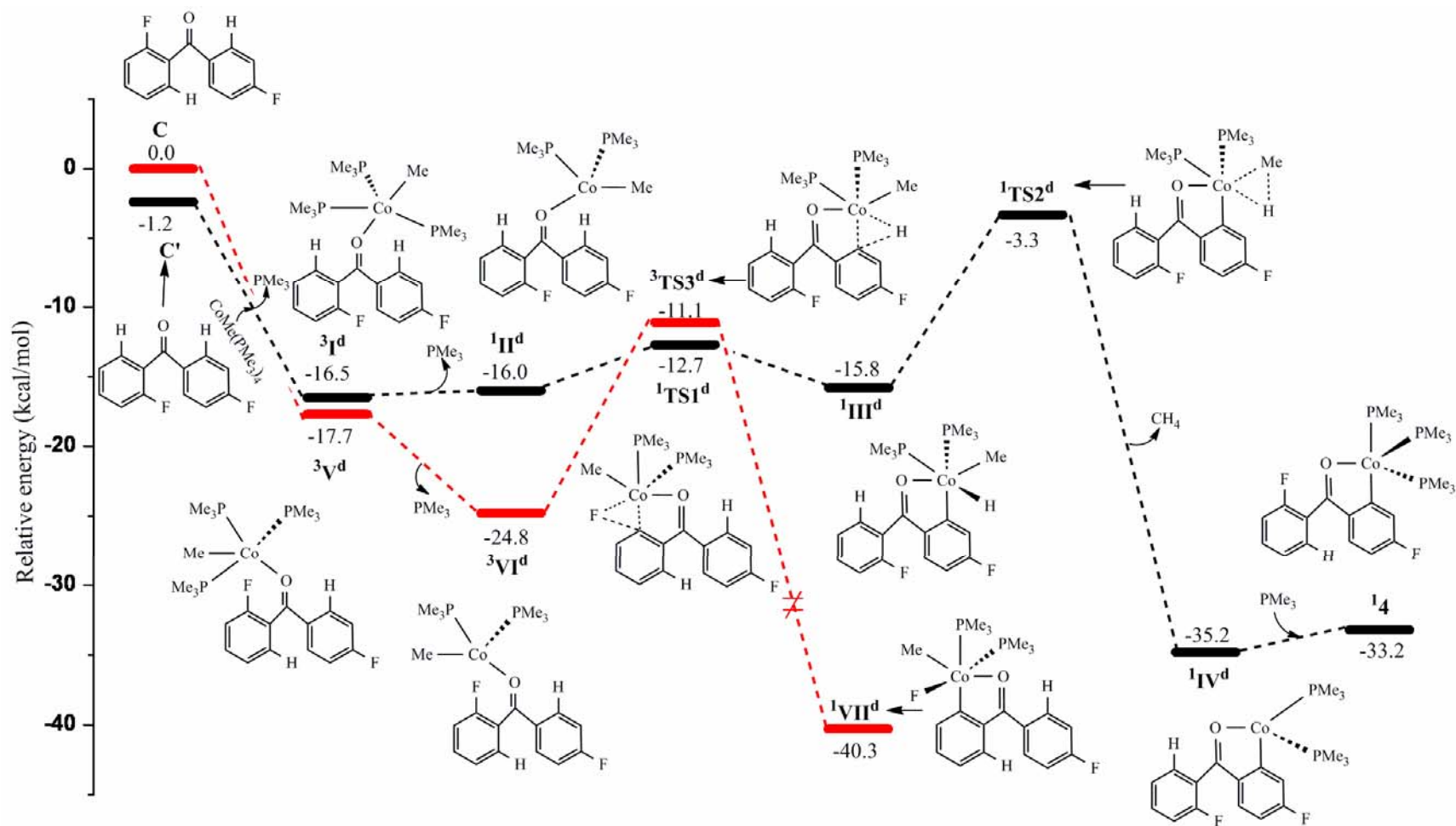


Fig. 7 Calculated free energy profiles for the reaction of $\text{CoMe}(\text{PMe}_3)_4$ with 2,4'-difluorobenzophenone (**C**) along both the *ortho* C-F activation pathway (red line) and the *ortho* C-H activation pathway (black line). The symbol \neq denotes the spin-crossover transition from the triplet surface to the singlet surface.

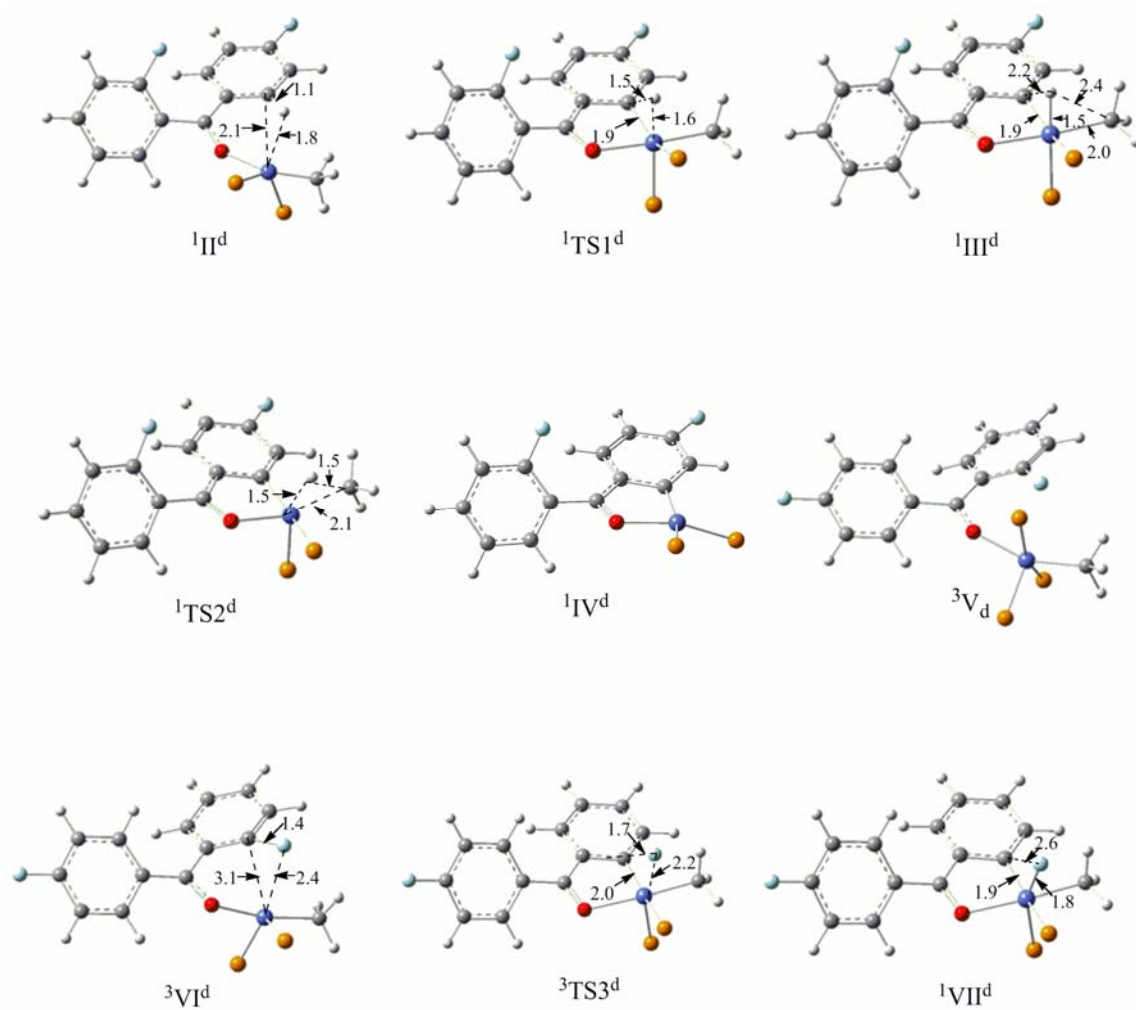
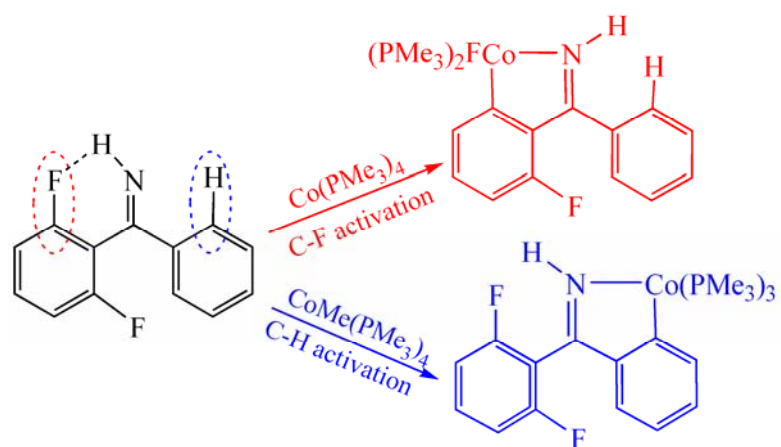


Fig. 8 Optimized structures with crucial geometrical parameters (in \AA) for all schematic structures involved in Fig. 7. The methyl groups on phosphorous atoms have been omitted for clarity, and bond distances are given in \AA

Table of Contents Graphic



The selective C-H and C-F activations of fluoroaromatic imines and ketones by cobalt complexes have been rationalized well by performing DFT calculations.